Argentobaumhauerite: name, chemistry, crystal structure, comparison with baumhauerite, and position in the Lengenbach mineralization sequence

DAN TOPA[1,*] AND EMIL MAKOVICKY[2]

[1] Natural History Museum-Wien, Burgring 7, 1010 Wien, Austria
[2] Institute for Geoscience and Mineral Resources Management, University of Copenhagen, Østervoldgade 10, DK-1350, Copenhagen K, Denmark

ABSTRACT

The crystal structure of argentobaumhauerite is reported for the first time from a sulfosalt aggregate from Lengenbach deposit, Binntal, Switzerland. The chemical formula of argentobaumhauerite, calculated in agreement with the results of structure determination is $Cu_{0.06}Ag_{1.20}Tl_{0.18}Pb_{21.46}Sb_{0.56}As_{32.28}S_{72.26}$. The difference from the idealized baumahuerite formula, $Pb_{12}As_{16}S_{36}$, and from the formula of Ag-, Tl- and Sb-free baumhauerite from Moosegg, Austria, $Pb_{11.80}As_{16.28}S_{35.92}$, expresses the Ag + As and Tl + As substitution for 2Pb. Argentobaumhauerite is triclinic, $a = 7.9053(10)$, $b = 8.4680(10)$, $c = 44.4102(53)$ Å, $\alpha = 84.614(2)$, $\beta = 86.469(2)$, $\gamma = 89.810(2)°$. V(cell) = 2954.16 Å^3, space group $P\bar{1}$. Baumhauerite $Pb_{11.80}As_{16.28}S_{35.92}$ from Moosegg is triclinic, $a = 7.884(4)$, $b = 8.345(4)$, $c = 22.811(11)$ Å, $\alpha = 90.069(8)$, $\beta = 97.255(8)$, $\gamma = 90.082(8)°$, V(cell) = 1488.8(13) Å^3, space group $P1$. Both minerals represent the $N_{1,2} = 3;4 = 3.5$ member of the sartorite homologous series, with As-rich slabs separated by zigzag layers of trigonal coordination prisms of lead. In argentobaumhauerite the sequence of alternating $N = 3$ and $N = 4$ slabs of baumhauerite is further modified by alternation of two distinct types of $N = 4$ slabs, those with Pb present in the slab interior and those with the interior Pb substituted by Ag + As. The length and arrangement of crankshaft chains of short As–S bonds differs between different slabs, and especially between the $N = 4$ slabs of baumhauerite and argentobaumhauerite. The name 'argentobaumhauerite' replaces the preliminary name 'baumhauerite-2a' (IMA-CNMNC; accepted proposal 15-F).

KEYWORDS: baumhauerite, argentobaumhauerite, crystal structure, Ag + As substitution, Tl + As substitution, mineralization sequence, Lengenbach.

Introduction

BAUMHAUERITE was discovered by Solly (1902) in a material from Lengenbach (Binntal, Switzerland) and named for the Freiburg professor Baumhauer who dedicated himself to the study of Lengenbach minerals. Baumhauerite is a Pb-As sulfosalt, a member of the sartorite homologous series. According to Makovicky (1985) this is a combinatorial series (Makovicky 1997a,b), in which only the members $N = 3$ and $N = 4$ are known, and the variety is created by combinations of these two unit homologue slabs in different ratios. Baumhauerite is the simplest of these combinations, namely $N_{1,2} = 3;4$.

The combined thickness of the alternating $N = 3$ and $N = 4$ slabs leads to the (010) spacing of ~22 Å for baumhauerite (Engel and Nowacki, 1969). The complications started by the discovery of two 'baumhauerite varieties', respectively silver-poor and silver-rich, by Laroussi *et al.* (1989). The discovery that the Ag-rich baumhauerite has a doubled *a* parameter, equal to 44.7 Å, by means of single-crystal X-ray photographs, confirmed by

*E-mail: dan.topa@nhm-wien.ac.at

electron diffraction, by Pring *et al.* (1990), was a further surprising complication of the baumhauerite problem. They suggested a monoclinic unit cell with $a = 44.74$, $b = 8.477$, $c = 7.910$ Å and $\beta = 93.37°$ with a possibility left open for a triclinic structure with α and γ close to 90° and named it 'baumhauerite-2*a*'. Two models are in agreement with the large unit cell – the $N_{1-4} = 3;4;3;4$ model or the $N_{1-4} = 3;3;4;4$ model – but which one corresponds to the structure of the mineral? In the first variation, what is the nature of the difference between the two consecutive 3;4 modules? Is it a differentiation of Pb, As and Ag as it was in general terms suggested by Pring *et al.* (1990)?

Pring and Graeser (1994) re-examined the problem more accurately and they suggest that baumhauerite is a polytypic series, with the '2*a*' member displaying a sequence of baumhauerite-like cells in which alternating cells are 'inverted about the *b* (i.e. 8 Å) repeat', whereas the unsubstituted baumhauerite has a sequence of cells without inversion. A new phase which they observed and studied by high-resolution transmission electron microscopy (HRTEM) and electron diffraction, '3*abc*', was interpreted by them as a 'normal-normal-reversed' sequence of 'baumhauerite cells'. The presence of cation substituents, especially Ag, should help to stabilize these polytypes. Besides giving an overall picture of the sartorite homologous series, as seen via HRTEM, Pring (2001) essentially summarizes the existing observations on baumhauerites.

The samples studied in the present work come from material collected between 1850 and 2011 at the Lengenbach quarry, Binntal, Switzerland. Altogether 152 samples were made available to us by the following persons (in chronological order): Peter Berlepsch (Switzerland), Horst Geuer (Germany), Frank Keutsch (Germany), Uwe Kolitsch (Austria), Thomas Raber (Germany), Phillippe Roth (Switzerland) and Ralph Cannon (Germany) from their private collections. As curator of the mineralogical collection, Uwe Kolitsch also provided selected material from 11 samples from the mineralogical collection of the Natural History Museum Vienna. The locality of the comparative material of substitution-free Pb-As baumhauerite is Moosegg by Golling, Salzburg Land, Austria, provided to the first author by Prof. Elisabeth Kirchner (Austria) in the mid 1990s, with chemistry and unit-cell parameters provided for the first time by Graeser *et al.* (1986).

The present study, especially because of the complete crystal structure determinations it contains, explains some of the previous observations and corrects some of their conclusions. The crystal structure of argentobaumhauerite is here compared with the refined structure of Ag-, Tl-, Sb-free baumhauerite. It also brings new knowledge concerning both the chemistry and deposition sequence of the sartorite homologues at the type locality of Lengenbach and the general features of the homologous series type of highly covalent and lone electron pairs (LEP).

The nomenclature voting proposal 15-F 'Renaming of baumhauerite-2*a* to argentobaumhauerite' was approved by the Commission on New Minerals, Nomenclature and Classification (CNMNC) of the International Mineralogical Association (IMA) by a vote 13-1 on May 13, 2015, stating that the independent status of argentobaumhauerite as a mineral species is beyond any doubt, based on its composition, symmetry, a detailed crystal structure and a clear compositional gap against baumhauerite.

Mineral chemistry

Up to twenty separate grains, depending on quantity of available material in a sample, were pre-lifted from the dolomite-based gangue containing sulfosalt aggregates and were embedded in an araldite mount, polished and studied in reflected light and examined by qualitative (back-scatter secondary electron (BSE) images and energy-dispersive spectroscopy analyses) and quantitative (wavelength-dispersive spectroscopy) electron microprobe analyses. This procedure was separately applied to all 152 samples.

Argentobaumhauerite, baumhauerite and the associated sulfosalts were analysed using a JEOL Hyperprobe JXA-8530F electron microprobe (installed at Natural History Museum, Vienna, Austria) operated at 25 kV and 20 nA, with a beam diameter of 2 µm. Wavelength-dispersion data were collected using the following standards and emission lines: galena (Pb*M*α), chalcopyrite (Cu*K*α), Ag metal (Ag*L*α), stibnite (Sb*L*α), cinnabar (Hg*L*α) and lorandite (Tl*L*α, As*L*α, S*K*α). The raw data were corrected for matrix effects with the JEOL on-line ZAF correction. The results of the electron microprobe analyses for baumhauerite and argentobaumhauerite are compiled in Table 1. Chemical data for associated sartorite homologues are not discussed in detail here, being the subject of other, separate, publications but are used for binary and ternary plots.

820

TABLE 1. Chemical data for the crystals investigated.

No.*	Sample	NA	Cu	Ag	Tl	Pb	Hg	Sb	As	S	total
1	argentobaumhauerite (Binn)	5	0.04(01)	1.38(08)	0.40(03)	47.38(13)	0.05(09)	0.72(05)	25.80(12)	24.72(02)	100.49(24)
2	baumhauerite (Binn)	4	0.02(01)	0.14(04)	0.39(04)	51.44(20)	0.06(05)	0.45(04)	23.74(04)	23.34(09)	99.58(16)
3	baumhauerite (Moosegg)	4	-	-	-	50.93(09)	-	-	25.40(09)	24.00(09)	100.33(05)

*[1] $Cu_{0.06}Ag_{1.20}Tl_{0.18}Pb_{21.46}As_{32.28}Sb_{0.56}S_{72.26}$ $\Sigma Ag + Tl + Cu = 1.44$, $\Sigma As + Sb = 32.84$, $N_{chem} = 3.55$, $Ag_{subs} = 29.1$, $Tl_{subs} = 1.5$, $ch = -1.29$, $ev = -1.14$
[2] $Cu_{0.01}Ag_{0.06}Tl_{0.09}Pb_{12.23}As_{16.28}Sb_{0.18}S_{35.82}$ $\Sigma Ag + Tl + Cu = 0.16$, $\Sigma As + Sb = 15.77$, $N_{chem} = 3.61$, $Ag_{subs} = 2.9$, $Tl_{subs} = 1.4$, $ch = 0.48$, $ev = 0.43$
[3] $Pb_{11.80}As_{16.28}S_{35.92}$ $N_{calc} = 3.45$, $Ag_{subs} = 0$, $Tl_{subs} = 0$, $ch = 0.91$, $ev = 0.81$
The compositions are expressed in wt.%. NA = number of analyses. Standard deviation for the last digit is shown in parentheses. The N_{chem} represents chemical calculated sartorite homologue number defined by Makovicky (1985) and Ag_{subs}, Tl_{subs} represent Ag and Tl substitution defined by Makovicky and Topa (2015). The parameters ch and ev express the absolute and relative error in the charge balance based on the sum of cation and anion charges.

The chemical formula of argentobaumhauerite from the Lengenbach quarry, calculated in agreement with the results of structure determination is $Cu_{0.06}Ag_{1.20}Tl_{0.18}Pb_{21.46}Sb_{0.56}As_{32.28}S_{72.26}$. The difference against the idealized baumhauerite formula, $Pb_{12}As_{16}S_{36}$, and against the formula of substitution-free baumhauerite from Moosegg, $Pb_{11.80}As_{16.28}S_{35.92}$, expresses the Ag + As and Tl + As substitution for 2Pb.

The homologue order N_{chem}, calculated for argentobaumhauerite from the results of chemical analysis according to the procedure given by Makovicky (1985) and Makovicky and Topa (2015), is 3.55, close to the structural value of 3.5. The percentage of the (Tl + (As,Sb)) substitution for 2Pb, in relation to a hypothetical end-member in which all Pb has been eliminated, is only 1.5%. The percentage of the (Ag + (As,Sb)) substitution for 2Pb, however, is very large, calculated as 29.1% of the theoretically possible substitution (which, unlike Tl, preserves the Pb sites in the trigonal coordination prisms).

Electron microprobe analyses of the studied samples of baumhauerite from Lengenbach, which is associated with argentobaumhauerite (Table 1) give $N = 3.61$, 1.4% of (Tl + (As,Sb)) substitution, and only 2.9% of (Ag + (As,Sb)) substitution for 2Pb. So, in principle, the typical baumhauerite is an unsubstituted or minimally substituted sartorite homologue $N = 3.5$.

Electron microprobe analysis of baumhauerite from Moosegg (Table 1) indicates that it is a pure Pb-As sulfosalt, $Pb_{11.80}As_{16.28}S_{35.92}$, N_{calc} = 3.45, without antimony, thallium and silver. This makes its crystal structure doubly interesting, because it allows one to investigate and specify unambiguously the nature of mixed cation positions, which is often not possible in cases of complex Pb-Tl-Ag-As-Sb compositions. This is also valuable for resolving the mixed positions in argentobaumhauerite.

When we compare our results with the published data, Laroussi et al. (1989) found between 1.4 and 2.1 wt.% Ag and 0 to 0.8 wt.% Tl in 'Ag-rich baumhauerite'; one analysis is given as $Pb_{10.54}Ag_{0.65}Tl_{0.10}As_{16.68}S_{36}$. In comparison, they found up to 0.8 wt.% Ag and 0.9 wt.% Tl; with Sb below 0.5 wt.%, in baumhauerite itself. They state that 'Ag-rich baumhauerite' forms 'lamellar intergrowth' with baumhauerite. Pring et al. (1990) found the average composition of baumhauerite-2a (now argentobaumhauerite) to be $Pb_{11}Ag_{0.7}As_{17.2}Sb_{0.4}S_{36}$, whereas the surrounding baumhauerite was $Pb_{12}As_{17.2}S_{36}$. The 2a phase occurred as irregular to flame-like inclusions in normal baumhauerite. Although there is no trace of diffuse streaking in the electron diffraction photographs of the baumhauerite varieties, Pring et al. (1990) demonstrate intergrowths of the two phases almost on a unit-cell level.

A compositional puzzle is represented by the structurally examined baumhauerite of Engel and Nowacki (1969), with symmetry and structure of baumhauerite but composition ($Pb_{11.6}As_{15.7}Ag_{0.6}S_{36}$) of argentobaumhauerite. The puzzle can be solved by inspecting their electron

TABLE 2. Single-crystal X-ray diffraction: experimental and refinement details.

	argentobaumhauerite (Binntal)	baumhauerite (Moosegg)
Crystal data		
Chemical formula	$Cu_{0.06}Ag_{1.20}Tl_{0.18}Pb_{21.46}As_{32.28}Sb_{0.56}S_{72.26}$	$Pb_{11.80}As_{16.28}S_{35.92}$
Structural formula	$Ag_{1.61}(Pb,Tl)_{20.75}As_{33.18}Sb_{0.46}S_{72}$	$Pb_{12.14}As_{15.86}S_{36}$
Chemical formula weight	9406	4839.2
Cell setting	Triclinic	Triclinic
Space group	$P\bar{1}$	$P1$
a (Å)	7.905(1)	7.884(4)
b (Å)	8.468(1	8.345(4)
c (Å)	44.410(5)	22.811(12)
α,β,γ (°)	84.614(2), 86.496(2), 89.810(2)	90.069(8), 97.255(8), 90.082(8)
V(Å^3)	2954.2(6)	1488.8(13)
Z	1	1
D_x (mg m^{-3})	5.29	5.4
No. of reflections for cell param.	7018	3217
μ (mm^{-1})	41.29	43.89
Crystal form	irregular	irregular
Crystal size (mm)	$0.05 \times 0.07 \times 0.13$	$0.05 \times 0.06 \times 0.16$
Crystal colour	black	black
Data collection		
T_{min}	0.1302	0.1496
T_{max}	0.4409	0.4147
No. of measured refl.	25,665	9902
No. of independent refl.	8445	6137
No. of obs. refl.	6545	5385
Criterion for obs. refl.	$I > 2(I)$	
R_{int}, R_{σ} (%)	7.09, 6.27	6.13, 8.46
θ_{max}(°)	23.28	20.96
Range of h, k, l	$-8 < h < 8, -9 < k < 9, -49 < l < 49$	$-7 < h < 7, -8 < k < 8, -22 < l < 22$
Refinement		
Refinement on F_o^2		
$R[F_o > 4\sigma(F_o)]$ (%)	3.94	5.00
$wR(F_o^2)$(%)	5.66	5.74
S (Goof)	0.995	1.00
No. of refl. used in refinement	8445	6137
No. of parameters refined	583	582
Weighting scheme	$w = 1/[\sigma^2(F_o^2) + (0.0318P)^2 + 0.0P]$ where $P = (F_o^2 + 2F_c^2)/3$	$w = 1/[\sigma^2(F_o^2) + (0.0464P)^2 + 0.0P]$
$(\Delta/\sigma)_{max}$	0.001	0.003
$\Delta\rho_{max}$ (e/Å^3)	3.46 [0.94 Å from Pb11]	1.37 [0.96 Å from As17]
$\Delta\rho_{min}$ (e/Å^3)	-3.40 [0.87 Å from Pb11]	-1.29 [0.91 Å from As17]
Extinction method	none	none
Source of atomic scattering factors:	*International Tables for Crystallography* (1992, Vol. C, Tables 4.2.6.8 and 6.1.1.4)	
Computer programs		
Structure solution	*SHELXS97* (Sheldrick, 1997*a*)	
Structure refinement	*SHELXL97* (Sheldrick, 1997*b*)	

microprobe data – only one analysis gave measurable Ag contents – and the total ensemble of four analyses suggests an unrecognized inclusion of argentobaumhauerite in a baumhauerite matrix. Thus, the material investigated was most probably as heterogeneous as that of the other investigators.

Crystallography, diffraction data collection and crystal structure analysis

For data collection (Table 2), fragments with irregular shape, removed from pre-analysed polished sections, were mounted on a Bruker AXS three-circle diffractometer equipped with a CCD area

TABLE 3*a*. Atom positions, occupancies (sof) and equivalent displacement parameters (Å^2) for argentobaumhauerite.

Atom	sof	x	y	z	U_{eq}
Pb1	1	0.28586(8)	0.41736(7)	0.877946(15)	0.03397(17)
Pb2	1	0.27922(8)	0.90572(7)	0.882129(15)	0.03181(17)
Pb3	1	0.19559(9)	0.58361(8)	0.168905(16)	0.04255(19)
Pb4	1	0.21902(8)	0.06641(7)	0.167892(15)	0.03392(17)
Pb5	1	0.01163(7)	0.72531(7)	0.739939(13)	0.02460(16)
Pb6	1	0.30778(8)	0.71939(7)	0.333626(14)	0.02952(16)
Pb7	1	0.29141(10)	0.21271(8)	0.333237(16)	0.0439(2)
Pb8	1	0.21333(8)	0.30861(7)	0.614997(14)	0.02870(16)
Pb9	1	0.21472(10)	0.80917(8)	0.613496(17)	0.0472(2)
Pb10	1	0.42344(8)	0.15308(7)	0.459424(14)	0.03036(17)
Ag	0.737(6)	0.05805(15)	0.62524(13)	0.04284(3)	0.0463(5)
Pb11	0.263(6)	0.05805(15)	0.62524(13)	0.04284(3)	0.0463(5)
As1	0.745(14)	0.0047(3)	0.0954(2)	0.03571(6)	0.0732(10)
Sb	0.255(14)	0.0047(3)	0.0954(2)	0.03571(6)	0.0732(10)
As2	1	0.3529(2)	0.1856(2)	0.97911(4)	0.0386(5)
As3	1	0.31844(19)	0.62005(17)	0.96874(3)	0.0243(4)
As4	1	0.3344(2)	0.84916(17)	0.08611(4)	0.0263(4)
As5	1	0.3202(2)	0.3007(2)	0.07944(4)	0.0369(4)
As6	1	0.2420(2)	0.1858(2)	0.80325(4)	0.0348(4)
As7	1	0.23543(19)	0.69897(16)	0.80925(3)	0.0207(3)
As8	1	0.07801(19)	0.77390(16)	0.24424(3)	0.0210(4)
As9	1	0.41758(18)	0.49937(16)	0.25375(3)	0.0170(3)
As10	1	0.42746(18)	0.08541(17)	0.24639(3)	0.0220(4)
As11	1	0.27809(18)	0.01650(16)	0.69074(3)	0.0176(3)
As12	1	0.25538(17)	0.45315(16)	0.69665(3)	0.0172(3)
As13	1	0.20103(18)	0.86874(17)	0.41665(3)	0.0219(4)
As14	1	0.18468(18)	0.42674(16)	0.41078(3)	0.0183(3)
As15	0.814(6)	0.4864(2)	0.6337(2)	0.46402(6)	0.0871(11)
Pb12	0.186(6)	0.4864(2)	0.6337(2)	0.46402(6)	0.0871(11)
As16	1	0.15130(18)	0.09072(16)	0.53384(3)	0.0193(3)
As17	1	0.1458(2)	0.6518(2)	0.52500(4)	0.0383(5)
S1	1	0.1706(5)	0.3198(4)	0.00778(10)	0.0307(10)
S2	1	0.1930(5)	0.9187(5)	0.01224(11)	0.0377(11)
S3	1	0.4947(5)	0.5702(5)	0.04357(12)	0.0411(12)
S4	1	0.4803(5)	0.8316(4)	0.94792(9)	0.0286(10)
S5	1	0.1864(5)	0.1728(4)	0.93890(9)	0.0248(9)
S6	1	0.1362(5)	0.6172(5)	0.93123(9)	0.0326(10)
S7	1	0.1475(5)	0.6503(5)	0.09754(9)	0.0319(10)
S8	1	0.1546(5)	0.0600(4)	0.09267(10)	0.0295(10)
S9	1	0.4507(5)	0.8334(4)	0.13132(9)	0.0265(9)
S10	1	0.4449(5)	0.3183(4)	0.12290(8)	0.0216(9)
S11	1	0.0747(4)	0.1771(4)	0.84672(8)	0.0207(8)
S12	1	0.0564(5)	0.6756(4)	0.85111(9)	0.0232(9)
S13	1	0.5927(5)	0.5063(4)	0.18093(9)	0.0219(9)
S14	1	0.3891(4)	0.9143(4)	0.82137(8)	0.0173(8)
S15	1	0.3088(5)	0.8065(4)	0.21110(9)	0.0246(9)
S16	1	0.2669(4)	0.2566(4)	0.21759(8)	0.0193(8)
S17	1	0.0841(5)	0.0231(4)	0.77619(9)	0.0256(9)
S18	1	0.0592(5)	0.4166(4)	0.77876(8)	0.0217(9)
S19	1	0.4352(4)	0.3027(4)	0.72518(8)	0.0200(8)
S20	1	0.4310(4)	0.7140(4)	0.72794(9)	0.0239(9)

(continued)

TABLE 3*a*. (*contd.*)

Atom	sof	x	y	z	U_{eq}
S21	1	0.1958(4)	0.4767(4)	0.28884(8)	0.0200(8)
S22	1	0.2307(4)	0.0155(4)	0.28370(8)	0.0188(8)
S23	1	0.1084(4)	0.2387(4)	0.68158(8)	0.0171(8)
S24	1	0.1100(4)	0.8303(4)	0.67692(8)	0.0196(8)
S25	1	0.4511(4)	0.0466(4)	0.64835(8)	0.0203(8)
S26	1	0.4211(4)	0.5191(4)	0.65488(8)	0.0201(8)
S27	1	0.0661(4)	0.9313(4)	0.37449(8)	0.0200(8)
S28	1	0.0420(4)	0.4512(4)	0.36822(8)	0.0208(8)
S29	1	0.3583(4)	0.6476(4)	0.40094(9)	0.0210(9)
S30	1	0.3685(4)	0.2404(4)	0.39803(8)	0.0207(8)
S31	1	0.0042(5)	0.7111(4)	0.44417(9)	0.0219(9)
S32	1	0.0084(5)	0.1202(4)	0.44711(9)	0.0265(9)
S33	1	0.3576(4)	0.0758(4)	0.56689(9)	0.0224(9)
S34	1	0.3197(5)	0.5992(4)	0.56313(8)	0.0223(9)
S35	1	0.3152(5)	0.8287(4)	0.49581(9)	0.0245(9)
S36	1	0.3004(5)	0.4222(5)	0.49411(10)	0.0330(10)

TABLE 3*b*. Atom positions, occupancies (sof) and equivalent displacement parameters (Å^2) for baumhauerite.

Atom		sof	x	y	z	U_{eq}
Pb1	Pb	1	−0.0089(2)	0.01268(18)	0.99844(8)	0.0294(5)
Pb2	Pb	1	0.9808(2)	0.51434(19)	0.99023(8)	0.0358(5)
Pb3	Pb	1	0.6984(2)	0.49627(18)	0.15199(8)	0.0277(5)
Pb4	Pb	0.636(11)	0.1937(3)	0.7219(3)	0.19332(13)	0.0493(12)
As17	As	0.364(11)	0.1937(3)	0.7219(3)	0.19332(13)	0.0493(12)
Pb5	Pb	1	0.8984(2)	0.24084(18)	0.32219(8)	0.0250(4)
Pb6	Pb	1	0.6244(2)	0.26403(19)	0.46932(9)	0.0380(5)
Pb7	Pb	1	0.6067(2)	0.75861(18)	0.46830(8)	0.0273(5)
Pb8	Pb	1	0.1532(2)	0.2583(2)	0.57444(9)	0.0377(5)
Pb9	Pb	1	0.1507(2)	0.76478(18)	0.57357(8)	0.0287(5)
Pb10	Pb	1	0.5486(2)	0.28028(18)	0.71480(8)	0.0238(4)
Pb11	Pb	1	0.4349(2)	0.01816(18)	0.89209(8)	0.0343(5)
Pb12	Pb	1	0.4629(2)	0.52600(19)	0.89826(8)	0.0385(5)
As1	As	1	0.4466(5)	0.2002(4)	0.06198(17)	0.0179(10)
As2	As	1	0.4177(5)	0.7548(5)	0.04936(19)	0.0202(10)
As3	As	1	0.1616(6)	0.2602(5)	0.1662(2)	0.0256(11)
As4	As	0.651(11)	0.7637(5)	0.9794(4)	0.15896(14)	0.0471(15)
Pb14	Pb	0.349(11)	0.7637(5)	0.9794(4)	0.15896(14)	0.0471(15)
As5	As	0.853(11)	0.8573(6)	0.7360(5)	0.2978(2)	0.050(2)
Pb13	Pb	0.147(11)	0.8573(6)	0.7360(5)	0.2978(2)	0.050(2)
As6	As	1	0.4633(5)	0.0126(5)	0.30790(18)	0.0182(10)
As7	As	1	0.4542(5)	0.4314(4)	0.29319(19)	0.0225(10)
As8	As	1	0.1563(5)	0.9421(4)	0.40859(18)	0.0180(10)
As9	As	1	0.1791(5)	0.5029(4)	0.41934(19)	0.0173(10)
As10	As	1	0.7468(5)	0.0132(4)	0.61743(19)	0.0185(10)
As11	As	1	0.7372(5)	0.5662(4)	0.62761(18)	0.0172(10)
As12	As	1	0.4959(5)	0.7633(4)	0.74489(19)	0.0198(10)

(continued)

TABLE 3b. (*contd.*)

Atom		sof	x	y	z	U_{eq}
As13	As	1	0.1285(5)	0.0633(5)	0.74188(19)	0.0276(11)
As14	As	1	0.1122(5)	0.4978(4)	0.72710(18)	0.0184(10)
As15	As	1	0.8650(5)	0.2701(5)	0.85143(18)	0.0201(10)
As16	As	1	0.8691(5)	0.7926(5)	0.83906(19)	0.0256(11)
S1	S	1	0.2616(13)	0.2461(12)	−0.0179(5)	0.027(3)
S2	S	1	0.2897(14)	0.0576(11)	0.1208(4)	0.024(3)
S3	S	1	0.2264(13)	0.7643(11)	−0.0310(5)	0.020(3)
S4	S	1	0.9063(15)	0.2395(14)	0.1091(6)	0.037(3)
S5	S	1	0.9294(13)	0.7702(11)	0.1091(5)	0.021(3)
S6	S	1	0.3232(13)	0.8010(12)	0.3529(5)	0.021(3)
S7	S	1	0.3338(13)	0.2299(11)	0.3480(5)	0.024(3)
S8	S	1	0.0172(12)	0.3068(11)	0.4456(4)	0.018(2)
S9	S	1	0.3779(13)	0.5085(12)	0.5001(5)	0.021(3)
S10	S	1	0.5744(12)	0.7907(10)	0.5951(5)	0.015(2)
S11	S	1	0.5632(12)	0.2056(12)	0.5871(5)	0.024(3)
S12	S	1	0.3059(13)	0.4989(11)	0.6621(5)	0.022(3)
S13	S	1	0.9519(12)	0.2925(12)	0.6867(5)	0.023(3)
S14	S	1	0.2825(13)	0.0196(11)	0.6668(5)	0.021(3)
S15	S	1	0.6496(13)	0.5569(11)	0.7907(5)	0.027(3)
S16	S	1	0.6700(11)	0.9626(10)	0.7878(4)	0.017(2)
S17	S	1	0.0295(12)	0.0429(10)	0.8757(4)	0.014(2)
S18	S	1	0.0452(12)	0.4672(11)	0.8768(5)	0.020(3)
S19	S	1	0.8857(13)	0.0056(11)	0.5369(5)	0.024(3)
S20	S	1	0.7459(12)	0.7684(10)	0.9235(4)	0.013(2)
S21	S	1	0.8607(13)	0.5213(11)	0.5470(5)	0.020(3)
S22	S	1	0.7196(14)	0.2672(12)	0.9296(5)	0.022(3)
S23	S	1	0.0215(12)	0.7221(11)	0.4431(4)	0.016(2)
S24	S	1	0.6073(15)	0.7526(14)	0.2300(6)	0.038(3)
S25	S	1	0.9960(14)	0.5306(12)	0.2440(5)	0.030(3)
S26	S	1	0.9956(13)	0.9747(13)	0.2440(5)	0.028(3)
S27	S	1	0.5802(13)	0.5612(10)	0.0239(5)	0.023(3)
S28	S	1	0.5919(14)	0.2664(11)	0.2365(5)	0.024(3)
S29	S	1	0.5831(12)	−0.0249(10)	0.0294(5)	0.018(2)
S30	S	1	0.9445(12)	0.7099(11)	0.6813(4)	0.018(2)
S31	S	1	0.2680(14)	0.4747(12)	0.1237(5)	0.028(3)
S32	S	1	0.3416(13)	0.9926(12)	0.4884(5)	0.023(3)
S33	S	1	0.6987(13)	0.0070(12)	0.3723(5)	0.020(3)
S34	S	1	0.3130(12)	0.2370(11)	0.7967(4)	0.017(2)
S35	S	1	0.2873(14)	0.7780(12)	0.8041(5)	0.025(3)
S36	S	1	0.6748(15)	0.4971(12)	0.3627(6)	0.034(3)

detector, respectively, for baumhauerite and argentobaumhauerite. The *SMART* (Bruker AXS, 1998*a*) system of programs was used for unit-cell determination and data collection, *SAINT+* (Bruker AXS, 1998*b*) for the reduction of the intensity data, and *XPREP* (Bruker AXS, 1997) for space-group determination and empirical absorption correction based on pseudo ψ-scans. The centrosymmetric space group $P\bar{1}$ proposed by the *XPREP* program for argentobaumhauerite was chosen. It is consistent

with the triclinic symmetry of the lattice and intensity statistics. The structure of argentobaumhauerite was solved by direct methods (Sheldrick, 1997*a*). The list of atom positions was completed in subsequent cycles of the refinement (Sheldrick, 1997*b*), by means of difference-Fourier syntheses. In the final stage of refinement all the positions were treated anisotropically. For baumhauerite the *P*1 space group was chosen. It is consistent with the triclinic symmetry of the lattice and intensity

TABLE 4a. Selected cation–ligand distances (in Å) in argentobaumhauerite.

Pb1–	Pb2–	Pb3–	Pb4–	Pb5–	Pb6–	Pb7–	Pb8–	Pb9–	Pb10–
S13 2.749(4)	S14 2.778(4)	S15 2.959(4)	S16 2.895(4)	S21 2.817(4)	S25 2.951(4)	S22 2.947(4)	S28 2.973(3)	S24 2.908(4)	S30 2.817(4)
S9 3.007(4)	S10 2.898(4)	S18 2.980(4)	S15 2.897(4)	S16 2.823(3)	S26 2.974(3)	S21 2.967(3)	S27 2.992(3)	S28 3.022(3)	S33 2.876(4)
S12 3.040(4)	S9 3.070(4)	S11 3.007(3)	S14 3.170(3)	S24 2.915(3)	S29 3.044(4)	S30 3.008(4)	S23 3.026(3)	S34 3.060(4)	S35 2.968(4)
S10 3.090(4)	S12 3.102(4)	S12 3.192(4)	S12 3.174(4)	S18 3.029(3)	S21 3.156(4)	S25 3.078(3)	S26 3.159(4)	S33 3.084(4)	S34 2.985(4)
S11 3.112(4)	S11 3.159(3)	S9 3.206(4)	S9 3.178(4)	S22 3.062(3)	S27 3.213(3)	S28 3.250(3)	S33 3.198(4)	S27 3.176(3)	S36 2.995(4)
S6 3.202(4)	S6 3.274(4)	S7 3.213(4)	S10 3.243(3)	S17 3.188(4)	S19 3.228(3)	S24 3.259(3)	S25 3.217(3)	S25 3.301(4)	S35 3.147(3)
S5 3.306(4)	S4 3.417(4)	S13 3.270(4)	S11 3.245(3)	S20 3.328(3)	S22 3.269(3)	S26 3.318(3)	S31 3.245(4)	S32 3.315(4)	S32 3.376(4)
S7 3.562(4)	S8 3.561(4)	S16 3.417(3)	S17 3.378(4)		S28 3.303(3)	S27 3.319(3)	S34 3.283(3)	S30 3.334(3)	
S3 3.998(5)	S5 3.583(4)	S10 3.667(4)	S8 3.415(5)		S23 3.410(3)	S20 3.397(4)	S29 3.431(3)	S26 3.401(3)	

Ag/Pb11	As1/Sb–	As2–	As3–	As4–	As5–	As6–	As7–	As8–	As9–
S7 2.599(4)	S2 2.372(5)	S1 2.241(4)	S3 2.241(4)	S7 2.264(4)	S10 2.245(4)	S11 2.238(4)	S13 2.267(4)	S15 2.230(4)	S21 2.269(4)
S6 2.694(4)	S1 2.499(4)	S5 2.293(4)	S6 2.293(4)	S9 2.270(4)	S4 2.252(4)	S17 2.286(4)	S12 2.325(4)	S17 2.260(4)	S20 2.278(4)
S5 2.713(4)	S2 2.730(5)	S3 2.494(4)	S4 2.494(4)	S8 2.293(4)	S8 2.307(4)	S18 2.431(4)	S14 2.620(4)	S18 2.317(4)	S19 2.298(4)
S2 2.892(4)	S5 2.836(4)	S2 2.835(4)	S1 2.835(4)	S4 3.127(4)	S3 3.275(4)	S14 2.952(5)	S18 2.653(4)	S22 3.218(4)	S16 3.109(4)
S1 2.973(5)	S8 2.849(5)	S4 3.536(4)	S2 3.536(4)	S3 3.432(5)	S7 3.358(5)	S13 3.400(5)	S17 3.079(4)	S21 3.249(4)	S15 3.225(4)
S1 3.237(4)	S6 3.126(5)	S4 3.563(4)	S3 3.563(4)	S2 3.670(5)	S1 3.527(5)	S15 3.452(5)	S20 3.569(4)	S23 3.831(4)	S13 3.434(4)
S3 3.483(4)	S4 3.916(5)	S2 3.728(4)	S3 3.728(4)	S5 3.890(4)	S6 3.890(4)	S19 3.723(4)	S19 3.748(4)		
							S9 3.892(4)		

As10–	As11–	As12–	As13–	As14–	As15/Pb12–	As16–	As17–
S22 2.241(3)	S24 2.219(4)	S26 2.232(4)	S27 2.232(4)	S30 2.230(4)	S36 2.546(4)	S33 2.256(4)	S34 2.258(4)
S16 2.278(4)	S25 2.253(4)	S19 2.271(4)	S31 2.274(4)	S28 2.253(4)	S36 2.596(5)	S32 2.258(4)	S35 2.270(4)
S20 2.443(4)	S23 2.326(4)	S23 2.331(4)	S29 2.380(4)	S29 2.316(4)	S35 2.596(4)	S31 2.330(4)	S32 2.645(4)
S15 3.131(4)	S20 3.191(4)	S20 3.094(4)	S32 2.991(4)	S32 3.201(4)	S34 2.809(4)	S35 3.142(4)	S36 2.727(5)
S14 3.259(4)	S19 3.272(4)	S24 3.444(4)	S30 3.427(4)	S31 3.228(4)	S33 2.938(4)	S36 3.349(4)	S31 3.429(4)
S19 3.597(4)		S21 3.642(3)	S33 3.649(4)	S36 3.863(5)	S29 3.029(5)		S36 3.747(4)
		S28 3.856(4)	S35 3.668(4)				
		S18 3.859(4)					

statistics. The structure of baumhauerite was solved by direct methods (Sheldrick, 1997a). In the final stage of refinement all positions were treated anisotropically and the atomic sites were re-labelled in concordance with site denomination in baumhauerite made by Engel and Nowacki (1969).

Single crystal diffraction data indicate that argentobaumhauerite is triclinic, $a = 7.9053(10)$, $b = 8.4680(10)$, $c = 44.4102(53)$ Å, $\alpha = 84.614(2)$, $\beta = 86.469(2)$, $\gamma = 89.810(2)°$, $V(\text{cell}) = 2954.16$ Å^3, space group $P\bar{1}$. In agreement with previous investigations, the c parameter is doubled against that of baumhauerite. The substitution-free Moosegg material is triclinic, $a = 7.884(4)$, $b = 8.345(4)$, $c = 22.811(11)$ Å, $\alpha = 90.069(8)$, $\beta = 97.255(8)$, $\gamma = 90.082(8)$, $V(\text{cell}) = 1488.8(13)$ Å^3, space group $P1$.

Complete experimental and refinement data for both minerals, argentobaumhauerite and baumhauerite, respectively, are given in Table 2. Atomic position parameters, refined occupancies and U_{eq} parameters are in Tables 3a and 3b, whereas tables of complete anisotropic displacement parameters (Tables 3c and 3d) have been deposited with the Principal Editor of Mineralogical Magazine and are available from ww.minersoc.org/pages/e_journals/dep_mat_mm.html). The bond distances are given in Tables 4a and 4b, and the polyhedron characteristics in Tables 5a and 5b.

Description of crystal structures

In agreement with its structure scheme, as a sartorite homologue $N_{1,2} = 3;4$, the crystal structure of argentobaumhauerite contains 28 cation sites and 36 sulfur sites. Only three cation sites, Ag–Pb11, As1–Sb and As15–Pb12, were refined as mixed sites. The lower symmetry of baumhauerite leads to the same number of independent positions, from which Pb4–As17, As4–Pb14 and As5–Pb13 are mixed sites. Because of the very large number of refined parameters, in both structures the same positional parameters were used for both cations which share a mixed site (Tables 3a,b). The details of the structures will be described according to the structure segments defined for sartorite homologues by Makovicky (1985). These are slabs of different thickness, all based on the SnS archetype, formed primarily by As coordination polyhedra with a crankshaft arrangement of the short As–S bonds, terminating in a zig-zag layer of Pb coordination polyhedra.

Both crystal structures (Figs 1a,b) contain one type of $N = 3$ slab built from arsenic coordination polyhedra with participation of Pb (Figs. 2a,b). It alternates regularly with $N = 4$ slabs. In the case of argentobaumhauerite there are two kinds of $N = 4$ slabs in alternation; these display different degrees of substitution of 'fundamental' cations, As and Pb, by Ag (Fig. 2b). They will be called the 'unsubstituted' and the 'substituted' kind of slab, respectively. In baumhauerite there is only one compositional type of $N = 4$ slabs. Both slab types are subdivided into tightly-bonded double-layers, typical for the sartorite homologues, which are formed by means of short As–S bonds. The double-layers are separated by broader spaces which accommodate the lone electron pairs of (especially) As.

In argentobaumhauerite, the $N = 3$ slab is composed of six distinct columns of cations: Pb3–Pb4, Pb6–Pb7, Pb5–As8, As6–As7, As9–As10 and As11–As12, with 8.5 Å periodicity. The As7, 8, 9, 11, 12 atoms form trapezoidal coordination pyramids with three typical short bond distances (Table 4a). They are alternatively bottom- and side-bonded in their pyramidal bases (Fig. 3). The bottom-bonded As10 has one of these distances extended to 2.44 Å; the extension is probably forced by the configuration of surrounding Pb coordination polyhedra and LEP of arsenic. The arsenic site As6 displays two short distances, 2.26 Å and 2.33 Å, whereas two more distances in the base of the coordination pyramid are longer and equal (2.62 and 2.65 Å long); they oppose one another. The As6 site is obviously a position flipping between the bottom-bonded and side-bonded orientation, averaging the short and long distances involved in the flip.

In the $N = 3$ slab, one side of the diagonally oriented tightly-bonded double-layer is composed of well-developed crankshaft chains S24–As11–S23–As12–S19–As9–S20–As10–S16; the third short bond of each of these As atoms bridges the double layer. Each crankshaft chain ends in the Pb4 polyhedron, whereas the alternating Pb3 polyhedron faces a gap between adjacent crankshaft chains (Fig. 3). The opposite side of the double layer has a very short chain S13–As7–S14–As6–S17–As8–S18, complicated by the presence of the flipping As6 position which alternates between the short As6–S17 bond and the short As6–S18 bond (Fig. 3); as already mentioned, both of these distances show the bond length averaged to ~2.6 Å. Among the associated Pb atoms, Pb5 faces a gap between adjacent crankshaft chains; because of this position, its polyhedron cross-section has a widely 'open' shape. In its 8.5 Å column, Pb5 alternates with As8. The Pb6 atom faces the As8

TABLE 4*b*. Selected cation–ligand distances (in Å) in baumhauerite.

Pb1–	Pb2–	Pb3–	Pb4–	Pb5–	Pb6–	Pb7–	Pb8–	Pb9–	Pb10–
S17 2.865(10)	S18 2.727(12)	S28 2.918(11)	S25 2.601(12)	S33 2.836(11)	S11 2.832(12)	S9 2.909(11)	S12 2.976(10)	S19 2.946(10)	S12 2.805(10)
S3 2.917(10)	S3 2.926(10)	S24 2.929(13)	S5 2.681(10)	S8 2.904(9)	S9 2.964(11)	S32 2.940(11)	S14 2.987(10)	S23 3.042(9)	S34 2.819(10)
S1 2.945(11)	S20 3.090(9)	S4 2.940(13)	S31 2.711(11)	S28 2.918(11)	S36 3.180(13)	S10 2.947(12)	S19 3.026(10)	S21 3.059(10)	S15 2.932(10)
S20 3.156(9)	S22 3.109(10)	S25 2.957(11)	S26 2.947(11)	S36 2.992(12)	S33 3.188(11)	S33 3.166(11)	S8 3.026(9)	S14 3.090(10)	S11 2.995(12)
S22 3.276(10)	S1 3.172(10)	S27 3.003(11)	S24 3.272(12)	S26 3.007(11)	S21 3.220(10)	S21 3.204(10)	S21 3.191(10)	S12 3.145(10)	S14 3.120(10)
S4 3.289(13)	S27 3.367(11)	S5 3.153(10)	S2 3.388(10)	S25 3.158(11)	S8 3.230(10)	S6 3.251(10)	S13 3.191(10)	S30 3.147(10)	S16 3.214(9)
S5 3.320(11)	S5 3.513(11)	S31 3.378(11)	S6 3.713(12)	S7 3.410(10)	S19 3.239(10)	S19 3.263(10)	S11 3.239(10)	S32 3.224(11)	S13 3.323(10)
S29 3.393(10)	S31 3.573(11)				S32 3.244(11)	S36 3.342(13)	S9 3.336(11)	S10 3.321(10)	
S2 3.436(10)	S4 3.657(13)				S7 3.374(11)	S23 3.405(10)	S32 3.422(11)	S9 3.369(11)	

Pb11–	Pb12–	As1–	As2–	As3–	As4–	As5–	As6–	As7–	As8–
S34 2.912(9)	S27 2.913(11)	S1 2.220(11)	S27 2.186(11)	S31 2.248(12)	S26 2.492(11)	S24 2.351(13)	S33 2.217(11)	S28 2.259(12)	S32 2.225(11)
S35 2.965(11)	S22 2.987(11)	S2 2.273(11)	S3 2.223(11)	S4 2.261(12)	S5 2.535(11)	S25 2.445(12)	S7 2.325(11)	S36 2.267(12)	S6 2.270(12)
S22 3.096(11)	S20 3.010(9)	S29 2.333(10)	S29 2.331(10)	S2 2.284(11)	S4 2.755(13)	S26 2.646(12)	S6 2.383(12)	S7 2.365(11)	S23 2.308(10)
S17 3.178(10)	S15 3.027(12)	S31 3.117(12)	S31 3.200(12)	S25 3.245(12)	S24 2.869(13)	S36 2.962(13)	S28 2.930(11)	S24 3.340(13)	S7 3.182(11)
S29 3.222(11)	S35 3.197(11)	S27 3.342(10)	S2 3.236(11)	S26 3.336(12)	S29 3.114(11)	S33 3.178(12)	S24 3.108(14)	S6 3.576(11)	S8 3.379(10)
S1 3.226(11)	S3 3.286(11)	S4 3.662(12)		S28 3.565(12)	S28 3.362(11)	S23 3.405(10)	S26 3.803(11)	S25 3.739(11)	S33 3.640(11)
S16 3.229(10)	S18 3.303(10)	S22 3.963(13)			S2 3.786(12)	S6 3.767(11)		S31 3.976(12)	S26 3.818(12)
S20 3.232(9)	S34 3.445(9)								
S3 3.316(11)	S1 3.521(11)								

As9–	As10–	As11–	As12–	As13–	AS14–	As15–	As16–
S8 2.204(10)	S11 2.215(10)	S21 2.218(12)	S35 2.259(13)	S14 2.251(12)	S13 2.253(10)	S18 2.200(10)	S20 2.273(11)
S9 2.263(11)	S19 2.255(13)	S30 2.257(11)	S15 2.284(10)	S34 2.305(10)	S12 2.259(12)	S22 2.238(13)	S16 2.322(9)
S23 2.315(10)	S10 2.317(9)	S10 2.340(9)	S16 2.293(9)	S13 2.598(11)	S30 2.374(10)	S17 2.326(10)	S17 2.526(9)
S7 3.135(11)	S13 3.143(11)	S13 3.056(10)	S14 3.137(10)	S35 2.970(11)	S34 3.024(10)	S15 3.155(10)	S15 2.754(10)
S6 3.196(11)	S30 3.226(10)	S11 3.384(11)	S12 3.154(10)	S17 3.249(11)	S35 3.135(11)	S16 3.236(9)	S18 3.124(10)
	S14 3.964(12)	S12 3.629(12)	S10 3.556(13)	S30 3.490(10)	S18 3.530(12)	S34 3.902(11)	S35 3.491(12)
		S9 3.825(11)		S16 3.977(10)		S13 3.908(12)	S30 3.784(11)
		S15 3.869(13)					S3 3.830(11)

TABLE 5a. Polyhedron characteristics for the refined structure of argentobaumhauerite.

Atom	1	2	3	4	5	6	7	8
Pb1	9	3.210	0.038	0.385	0.783	138.507	65.206	2.0
Pb2	9	3.202	0.019	0.359	0.950	137.572	66.027	2.0
Pb3	9	3.205	0.010	0.292	0.921	137.938	66.856	1.7
Pb4	9	3.178	0.028	0.172	0.876	134.497	63.968	1.9
Pb5	7	3.042	0.096	0.246	0.913	117.933	40.333	2.2
Pb6	9	3.167	0.019	0.198	0.936	133.042	63.886	1.8
Pb7	9	3.171	0.021	0.041	0.840	133.551	63.985	1.8
Pb8	9	3.165	0.018	0.198	0.946	132.825	63.828	1.8
Pb9	9	3.173	0.015	0.115	0.859	133.800	64.468	1.8
Pb10	7	3.040	0.088	0.216	0.885	117.711	40.637	2.1
Ag/Pb11	7	2.965	0.109	0.404	0.857	109.230	36.822	1.1
As1/Sb	7	2.875	0.096	0.597	0.770	99.530	34.046	2.1
As2	7	2.950	0.120	0.711	0.872	107.545	35.797	2.8
As3	6	2.864	0.125	0.713	0.922	98.391	27.390	3.0
As4	7	2.939	0.080	0.751	0.856	106.350	37.041	3.1
As5	7	2.879	0.105	0.708	0.925	99.953	33.862	2.9
As6	8	2.974	0.057	0.684	0.675	110.138	45.026	2.7
As7	6	2.897	0.123	0.748	0.882	101.862	28.436	3.1
As8	6	2.775	0.080	0.643	0.962	89.538	26.212	3.0
As9	6	2.751	0.086	0.628	0.966	87.176	25.354	3.0
As10	6	2.891	0.176	0.696	0.926	101.209	26.550	2.8
As11	5	2.780	0.290	0.671	0.983	89.984	13.206	3.1
As12	8	3.042	0.070	0.738	0.680	117.868	47.517	3.1
As13	7	2.914	0.100	0.729	0.906	103.652	35.312	3.0
As14	6	2.870	0.113	0.734	0.865	99.068	27.969	3.1
As15/Pb12	6	2.760	0.061	0.287	0.972	88.067	26.318	1.8
As16	5	2.826	0.338	0.683	0.983	94.586	12.938	3.0
As17	6	2.894	0.168	0.674	0.940	101.523	26.887	2.7

See foot of Table 5b for key.

polyhedron via a long S–S edge whereas Pb7 faces Pb5 via a relatively short S–S edge (Fig. 3).

Across the thickness of the tightly-bonded double layer, the crankshaft chains are faced by Pb polyhedra, which participate in the composition of the double layer and are situated on its opposite surface. There are no short As–S bonds interconnecting the crankshaft chains on the two faces of the same double layer, which also differ substantially and are orientated perpendicular to one another. The slab of $N = 3$ double layers is not on elements of symmetry; it is asymmetric and the inversion centres of the $P\bar{1}$ space group are situated in, and between, double layers of the two kinds of $N = 4$ slabs.

The $N = 3$ slab in baumhauerite bears a close resemblance to that in argentobaumhauerite (compare Fig. 4 and Fig. 3). The four-member crankshaft chain S34–As13–S13–As14–S30–As11–S10–As10–S11, with additional short bonds As–S orientated to the opposite face of a

double layer, corresponds fully to the four-member chain in argentobaumhauerite. The short chain on the opposing surface of the double-layer, S18–As15–S17–As16–S16–As12–S15 with side bonds, is analogous to the short chain in argentobaumhauerite but it is a typical crankshaft arrangement because its As16 position lacks the flipping character. Instead, As16 has a scheme 2.53 Å *vs.* 2.75 Å, and As16 has an elongate bond 2.53 Å in the same position as in argentobaumhauerite.

The 'unsubstituted' $N = 4$ slab in argentobaumhauerite contains an inversion centre and consists of the 8.5 Å columns of coordination polyhedra As13–As14, As16–As17, Pb10–As15 and Pb8–Pb9 (Fig. 5, right-hand side). The As13, As14, As16 atoms have typical As coordinations (Table 4a). However, As17 has a 2.26 Å bond to S34 in the vertex of the coordination pyramid, 2.27 Å to S35 in the base of the pyramid, and two almost equal longer bonds in the pyramidal base,

TABLE 5b. Polyhedron characteristics for the refined structure of baumhauerite.

Atom	1	2	3	4	5	6	7	8
Pb1	9	3.173	0.022	0.260	0.908	133.766	64.030	1.93
Pb2	9	3.230	0.015	0.386	0.953	141.165	68.014	1.92
Pb3	7	3.044	0.076	0.162	0.868	118.096	41.305	2.01
Pb4	7	3.054	0.113	0.492	0.823	119.338	40.079	2.85
Pb5	7	3.042	0.077	0.248	0.908	117.933	41.182	2.10
Pb6	9	3.161	0.013	0.155	0.885	132.293	63.873	1.89
Pb7	9	3.154	0.018	0.235	0.930	131.377	63.156	1.94
Pb8	9	3.149	0.015	0.124	0.869	130.782	63.046	1.90
Pb9	9	3.142	0.015	0.174	0.937	129.934	62.639	1.89
Pb10	7	3.043	0.092	0.266	0.926	118.066	40.587	2.15
Pb11	9	3.148	0.020	0.142	0.912	130.702	62.651	1.88
Pb12	9	3.179	0.005	0.256	0.894	134.577	65.523	1.85
As1	7	2.951	0.103	0.715	0.658	107.689	36.556	3.09
As2	5	2.755	0.294	0.673	0.992	87.582	12.793	3.30
As3	6	2.975	0.177	0.761	0.894	110.290	28.886	3.12
As4	7	2.974	0.078	0.558	0.900	110.171	38.455	1.63
As5	7	2.937	0.076	0.597	0.804	106.076	37.089	2.04
As6	6	2.912	0.168	0.738	0.794	103.451	27.409	2.96
As7	7	3.039	0.115	0.766	0.864	117.534	39.349	2.85
As8	7	2.944	0.104	0.757	0.897	106.912	36.236	3.12
As9	5	2.731	0.291	0.645	0.997	85.337	12.512	3.19
As10	6	3.044	0.307	0.794	0.655	118.149	26.072	3.18
As11	8	3.037	0.080	0.732	0.671	117.340	46.817	3.15
As12	6	2.767	0.086	0.649	0.970	88.735	25.803	3.07
As13	7	2.951	0.098	0.709	0.916	107.669	36.749	2.57
As14	6	2.761	0.101	0.631	0.953	88.194	25.232	3.01
As15	7	2.971	0.132	0.749	0.681	109.879	36.090	3.26
As16	8	2.986	0.072	0.672	0.659	111.510	44.859	2.73

[1] Coordination number; [2] radius r_s in Å of a circumscribed sphere, least-squares fitted to the coordination polyhedron; [3] 'volume-based' distortion $v = [V(\text{ideal polyhedron}) - V(\text{real polyhedron})]/V(\text{ideal polyhedron})$; the ideal polyhedron has the same number of ligands; [4] 'volume-based' eccentricity $ECC_V = 1 - [(r_s - \Delta)/r_s]^3$; Δ is the distance between the centre of the sphere and the central atom in the polyhedron; [5] 'volume-based' sphericity $SPH_V = 1 - 3\sigma_r r_s$; σ_r is a standard deviation of the radius r_s; [6] volume in Å^3 of the circumscribed sphere; [7] volume in Å^3 of coordination polyhedron; [8] bond-valence sum.

2.64 Å and 2.73 Å, which indicate flipping inside the coordination polyhedron. Flipping is apparently connected with the statistical occupancy of the immediately adjacent mixed site, modelled as 0.81 As15 and 0.19 Pb12, which has the shortest bonds markedly longer than the As–S bonds, and equal to 2.54 Å and 2 × 2.60 Å. The cigar-shaped anisotropic displacement ellipsoid of this site is oriented symmetrically in the pyramidal base and describes the mix of the more asymmetric As position with a more symmetrical Pb position. The As17 and As15 coordination polyhedra share a short 3.45 Å S–S edge. The flipping As17 site is the end-site of a crankshaft chain S30–As14–S29–As13–S31–

As16–S32–As17–S35 (or –S36 as another short-bonded alternative) which eventually can continue with the As15 position. The Pb10 polyhedron alternating with the As15 site copies, to a modest degree, the trapezoidal configuration of surrounding polyhedra but the polyhedra in the adjacent Pb8–Pb9 column have fairly regular cross-sections. The Pb8–Pb9 column completely backs the just defined crankshaft chain, which is two columns broad, but situated on the opposite face of the double layer, as dictated by the inversion centre in the double layer.

The 'substituted' $N = 4$ slab is centrosymmetric as well (Fig. 5, left-hand side). It is composed by
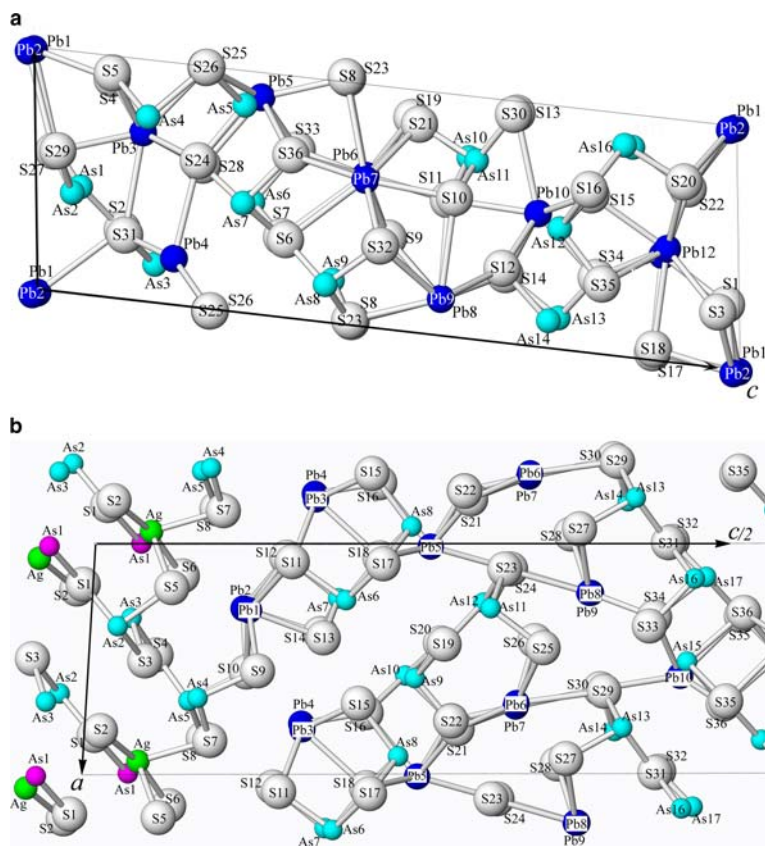
FIG. 1. Atom labels for the crystal structure of (*a*) baumhauerite and (*b*) argentobaumhauerite.

columns As4–As5, As2–As3, 'As1'–'Ag' and Pb1–Pb2. In this slab, only the first, marginal column is backed by Pb1 and Pb2 whereas the silver-containing polyhedral columns back one another, except for a side-shift of half-polyhedron width.

The composition of the crankshaft chain is S7–As4–S8–As5–S4–As3–S3–As2–S1; the chain continues to 'As1'–S2 and 'Ag'. In the perpendicular projection of the double layer, the crankshaft chains on the opposite sides of the double layer are antiparallel and continue one into another without a side-shift. Thus, the interspaces between crankshaft chains in the interior of one double layer, so-called secondary lone electron-pair micelles (primary micelles are the large interspaces between adjacent double layers), are continuous across the thickness of the double layer (Fig. 5), and participate in the accommodation of lone electron pairs. The corresponding situation in the unsubstituted layer was much less definite because of the heavy backing of crankshaft chains

by Pb polyhedra. There are no short As–S bonds interconnecting chains on the two faces of the 'substituted' double layer (the bridging As1–S2 bond is 2.73 Å long) and only an elongate, mixed-cation bond of this kind, As15–S36, is found in the 'unsubstituted' double-layer.

The arsenic sites As2 to As5 in the substituted layer have typical coordinations with three short cation–sulfur distances (Table 4*a*) whereas the sites 'As1' and 'Ag' are mixed sites for which the individual occupancies had to be modelled, considering the refined electron count and satisfying a stoichiometry of the mineral. The 'As1' site has been refined as 0.74 As mixed with 0.26 Sb, with the same set of positional coordinates and the same anisotropic displacement parameters. The shortest observed cation–anion distance is 2.37 Å to S2, and, together with the next short distance 2.50 Å to S1 (both situated in the base of the coordination pyramid), it is in agreement with the cation assignment. The two distances perpendicular to the
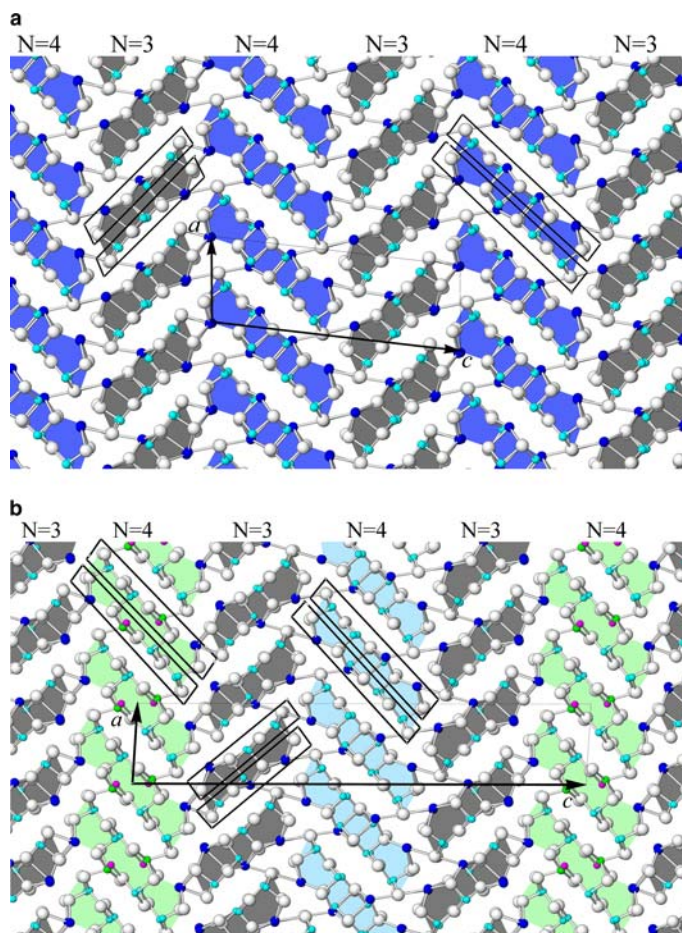
831

FIG. 2. Comparison of fundamental elements of the crystal structures of (*a*) baumhauerite and (*b*) argentobaumhauerite. The $N = 3$ and $N = 4$ slabs are divided into double-layer ribbons with tricapped trigonal coordination prisms of Pb at their obtuse ends, and As- and LEP-based interior portions (coloured). The $N = 3$ slabs are dark grey in both structures, whereas As-Pb saturated $N = 4$ layers are cyan in the argentobaumhauerite structure, and Ag-As rich $N = 4$ layers in this structure are light green. Baumhauerite has only one kind of $N = 4$ slab (Pb rich). Boxes indicate sites of crankshaft chains defined in the text for each ribbon.

trapezoidal cross-section, 2.73 Å and 2.85 Å, to S2 and S8, respectively, at the first sight do not agree with such an assignment. However, the enormous U^{33} value of the site (Table 3*c,d* deposited) probably suggests that this site is split into alternative sub-sites (chiefly within the base of the pyramid and also to a lesser degree along the S2–S8 line); these alternative sub-sites might even be bound to the alternative double layers. The nature of the major substituent, As, follows from the refinement but that of the minor 'Sb' substituent is not directly confirmable.

The 'Ag' site was modelled and refined as 0.74 Ag and 0.26 Pb, with the set of distances,

2.60 Å and longer (Table 4*a*), which simulate a distorted, irregular tetrahedral bond set. The linear coordination sometimes observed for Ag is absent (here 2.60 Å is opposed by 2.97 Å, to S7 and S1, respectively, and 2.69 Å is opposed by 2.89 Å, respectively to S6 and S2). The mixed Ag-Pb site displays a good Ag bond valence (BV) value of 1.1, supporting the assignment of silver. Its bonds/ distances show similarities to those of silver sites, Me7, 17 and 26 in the crystal structure of jasrouxite which contains a number of different types of Ag coordinations (Makovicky and Topa, 2014). Correlation of partial occupancies in the
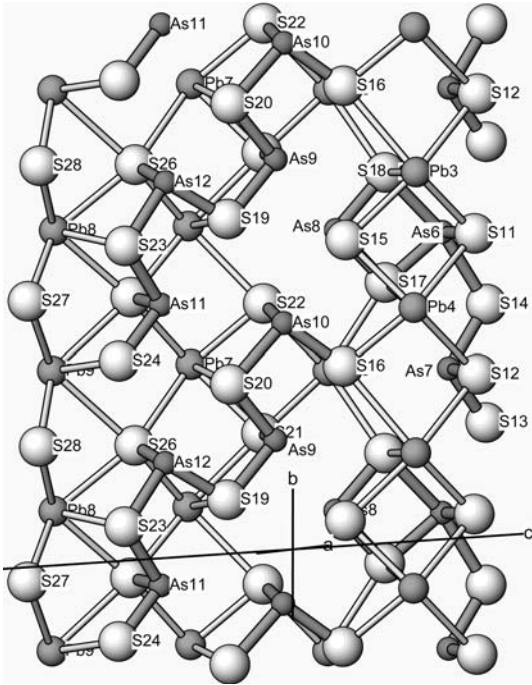
FIG. 3. A slightly oblique view of the $N = 3$ double layers in the crystal structure of argentobaumhauerite. Large white spheres: S; intermediate grey spheres: Pb; small grey spheres: As; black spheres: Ag; and dark sticks: short As–S bonds.
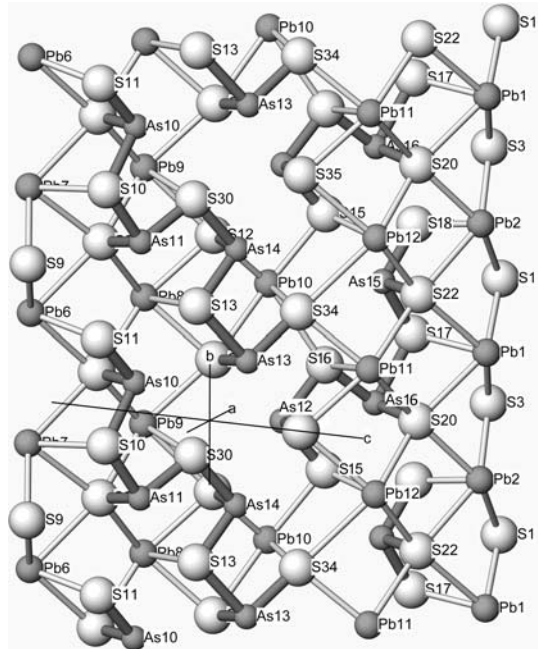
FIG. 4. A slightly oblique view of the $N = 3$ double layer in the crystal structure of baumhauerite. For conventions see Fig. 3.
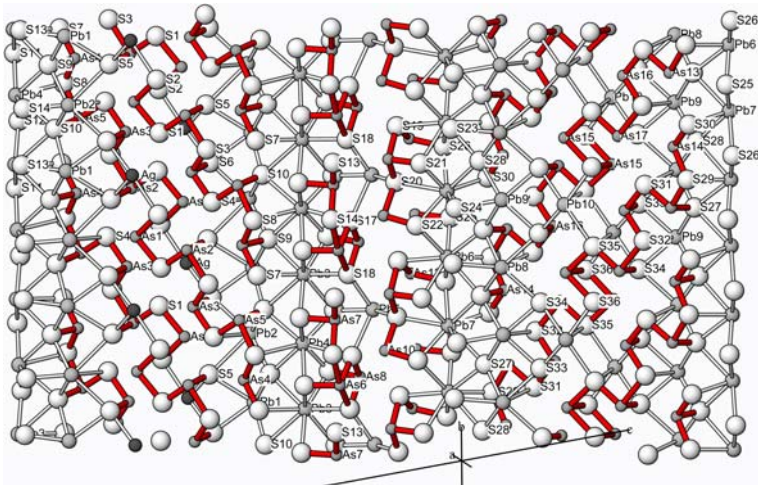

FIG. 5. A slightly oblique view of the $N = 4$ double layers in the crystal structure of argentobaumhauerite. From left to right: Configuration and As–S crankshaft chains in the substituted $N = 4$ slab, a nearly perpendicular view of the $N = 3$ slab, and the elements of the unsubstituted $N = 4$ slab. Large white spheres: S; intermediate grey spheres: Pb; small grey spheres: As; black spheres: Ag; and dark sticks: short As–S bonds.

833

'Ag' and 'As1' sites (Table 3a) is remarkable. The actual Ag–As–Sb–Pb mixing scheme at these two sites can be more complex than the trend modelled here.

The trigonal prismatic sites Pb1 and Pb2 (coordination number (CN) = 9) show prominent eccentricity (Table 5a), which is much lower for the rest of such Pb sites in the structure. Together with Pb3, they show the largest radius of circumscribed sphere and polyhedron volume. The As sites show uniformly large eccentricity. Large sphericity values, low distortion coefficient and uniform eccentricity values indicate that a description of As coordination polyhedra as CN = 6 and 7 polyhedra instead of CN = 3 polyhedra is a very appropriate, natural approach: the LEPs present about the same degree of steric activity for all As sites.

The Pb3 site has the lowest bond valence value (1.7) – it might be a possible Tl site. The arsenic sites are tolerably close to BV of 3.0 (Table 5a), except for the mixed sites As1 and As15, which have polyhedra larger than expected for pure As and show lower BV values as a consequence of it. Those arsenic sites which have coordinations somewhat deviating from the ideal set of three, about equally short, distances, have bond valence values 2.8, and even 2.7 for more severe cases (As6 and As17). The low BV values for sulfurs are all concentrated around the 'Ag' and 'As1' sites with intense cation substitution and, as S36, next to the substituted site 'As15'.

The N = 4 slab of baumhauerite displays configurations different from that of argentobaumhauerite. It contains a four-member crankshaft chain S8–As9–As8–S6–As6–SS7–As7–S28 with the additional short bonds oriented into the double layer. Its continuation is stopped by the Pb3 position (Fig. 6). On the opposing side of the double-layer, and perpendicular to the just described chain, a short chain is developed, comprising S27–As2–S29–As1–S2–As3–S31. All of these As atoms display typical coordinations with three short As–S bonds of about equal length (Table 4b).

Sandwiched between the chain systems of the N = 3 slab, and comprising the entire thickness of the double layer, is a cluster of mixed sites, designated as As4 (with 0.35 Pb), As5 (with 0.15 Pb) and Pb4(with 0.36 As) (Table 3b). The cation–S distances are correspondingly modified (Table 4b) and anisotropic displacement ellipsoids express the mixed character of the site. Except for the (As,Pb)4 site, however, no signs of flipping cation positions were seen.
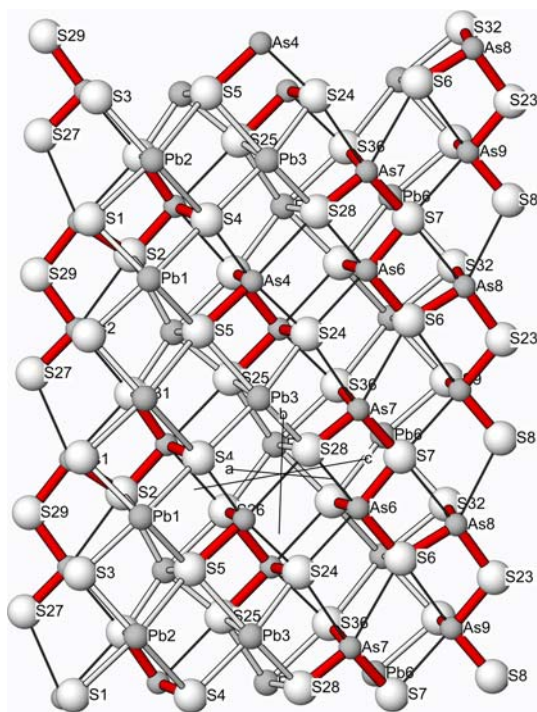

FIG. 6. A slightly oblique view of the N = 4 double layer in the crystal structure of baumhauerite. For conventions see Fig. 3.

Comparison of argentobaumhauerite and baumhauerite

The unit cell of argentobaumhauerite is related to that of baumhauerite as follows:

$$\mathbf{a} = \mathbf{a}, \mathbf{b} = \mathbf{b}, \mathbf{c} = 2\mathbf{c} - \mathbf{a} + \mathbf{b}/2$$

A simpler choice of argentobaumhauerite crystal axes, closer to the baumhauerite geometry, but less satisfactory from the formal point of view, is also possible, as indicated already by Pring et al. (1990).

The consecutive asymmetric N = 3 double layers are all orientated identically in baumhauerite (Fig. 4) whereas they are orientated alternatively along + a and –a in argentobaumhauerite (Fig. 3), as dictated by the inversion centres situated in the N = 4 slabs (Fig. 5). The orientation of chains in N = 3 slabs in respect to those in the 'low-Pb' face of the N = 4 double layers in baumhauerite is the same as for the unsubstituted slabs in argentobaumhauerite. The N = 4 low-Pb face in baumhauerite approximates in its occupancy, although not in all configurations, the faces of the double layers in the N = 4 unsubstituted slab of

argentobaumhauerite. The argentobaumhauerite cell ends up by 4.18 Å 'higher' along the 8.46 Å (=b) direction after the full 44.4 Å c period; this does not happen in the baumhauerite after the 22.8 Å c period. As already mentioned, the configuration of cation species is nearly the same in the $N = 3$ layers of baumhauerite (Fig. 4) as it is in argentobaumhauerite (Fig. 3). In both structures, the two kinds of chains on the opposing faces of the $N = 3$ double-layer are perpendicular to one another.

Investigating the width of blocks in the two structures, we measured the suitable cation–cation and S–S distances across the individual blocks, preserving the 'height' of atoms we use in relation to the 8.5 Å direction. The width of the $N = 3$ slab, expressed as the S11–S23 distance in argento-baumhauerite, is 10.89 Å, whereas when it is expressed as the As11–Pb4 distance, it is 7.61 Å. The corresponding distances in baumhauerite are S10–S20, which makes 11.14 Å (As10–Pb11 equal to 7.75 Å). The $N = 4$ slabs have widths S28–S29 equal to 14.59 Å (As14–Pb8 equal to 11.49 Å) in the unsubstituted slab of argentobaumhauerite, and S8–S9 equal to 14.36 Å (As4–Pb2 equal to 11.36 Å) in the substituted slab. In baumhauerite, these distances are S3–S23 equal to 15.27 Å (As6–Pb2 equal to 12.30 Å). As for the unit-cell volume, that of argentobaumhauerite is 2954.2 Å^3 whereas two times the unit-cell volume of baumhauerite is 2977.6 Å^3.

Thus, the baumhauerite structure is expanded when compared to argentobaumhauerite, even in the portions not directly involved in the Ag + As – for – 2Pb substitution. One consequence of relative compression is the appearance of flipping As positions in the structure of argentobaumhauerite, which are absent in the more expanded versions of the slab motif in baumhauerite.

The tightly-bonded double layer in dufrénoysite, $N = 4$, (Marumo and Nowacki 1967) is asymmetric, with crankshaft chains on the opposite faces perpendicular to one another. One side has a four-member chain, the other face has a three-member chain. A grouping of two (Pb,As) sites in the central part of the slab is similar but not identical to that in the $N = 4$ slab of baumhauerite.

The tightly bonded double layer in rathite $N = 4$ (Marumo and Nowacki 1965) has four-member chains, followed by an Ag position; Ag alternates in its column with Pb6; the last column are the trigonal prismatic sites Pb1–Pb2. Interestingly, the ultimate As position at the inner end of the chain has an elongated As–S bond of 2.68 Å, opposed by a distance of 2.71 Å, similar to the situation observed in argentobaumhauerite.

Concerning the chain orientations, Makovicky (1985) and Berlepsch *et al.* (2001) have noted previously that the orientation of crankshaft chains on the opposing sides of tightly-bonded double layers differs between the unsubstituted members ($N > 3$) and the corresponding Ag-substituted ones; at that time the latter category only contained rathite. The chains were usually shorter and perpendicular to one another in the former category and longer and parallel with one another, in the latter category. In baumhauerite, the chains on opposing sides of a double layer, both for the $N = 3$ and $N = 4$ slabs, run perpendicular to one another, although they are not identical because of the lacking intraslab symmetry (Figs 4, 6). In argentobaumhauerite, the perpendicular orientation of chains is preserved in the $N = 3$ slabs but in both types of $N = 4$ slabs the crankshaft chains on the two surfaces of the double layer are (anti)parallel, related by an inversion centre in the double layer. In addition, in the adjacent, non-equivalent (i.e. the substituted *vs.* the unsubstituted) $N = 4$ slabs, they slope in the opposing directions (Fig. 5), producing the effect observed by Pring and Graeser (1994) in HRTEM images and described by them as a 'reversal of the baumhauerite cell' (see the Introduction section). Thus, the baumhauerite–argentobaumhauerite pair parallels the dufrénoysite–rathite pair in the configuration of the arsenic-based chains and of entire slabs.

Position of baumhauerite varieties in respective mineralizations

Among the examined set of samples enumerated above, we found 36 samples contained argento-baumhauerite and argentobaumhauerite associations with other sartorite homologues. Eight of them were pure baumhauerite–argentobaumhauerite aggregates. They displayed prominent, fine to medium-coarse lamellar and spindle-like exsolutions of argento-baumhauerite from baumhauerite (Fig. 7*b*). Two systems of exsolution lamellae at oblique angles to one another are common. In BSE photographs, the argentobaumhauerite lamellae are distinctly darker than baumhauerite. Based on optical behaviour, the details of lamella orientation might differ from the matrix although the exsolution lamellae show a structurally determined shape. The single case representing exsolution of baumhauerite from argentobaumhauerite, in the form of thin spindles, thick irregular spindles, accumulations along grain boundaries, as well as half-spindles and
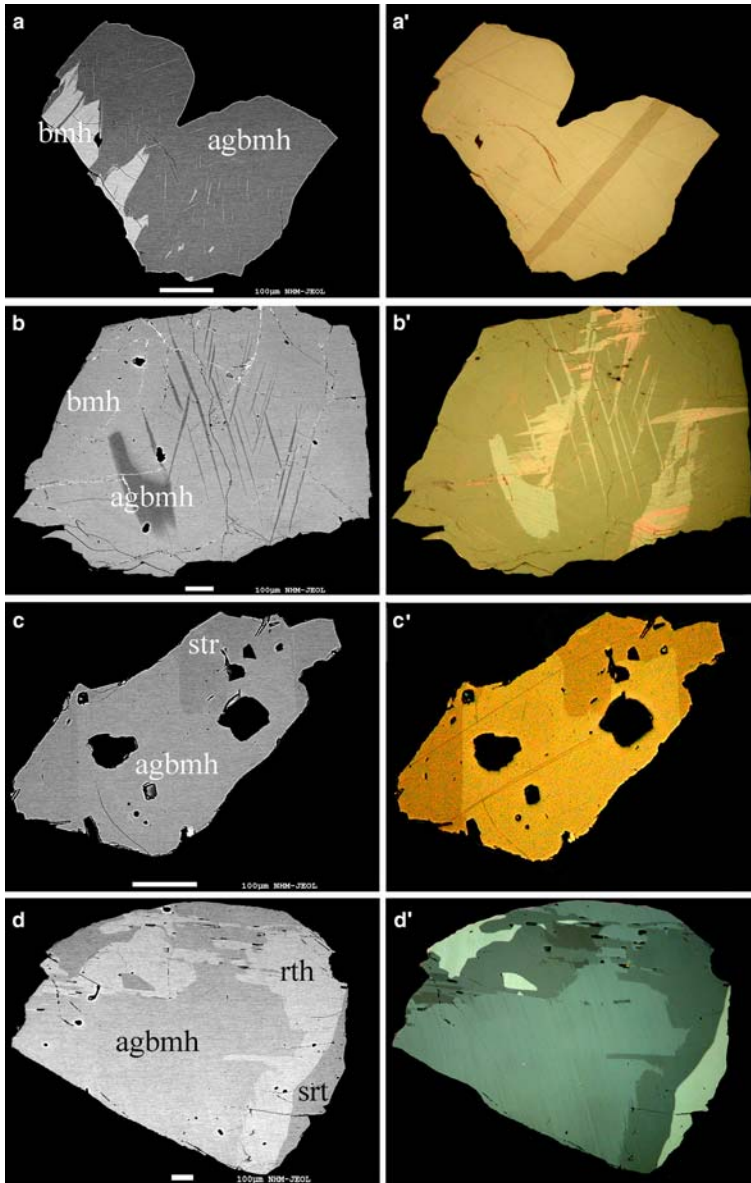
835

FIG. 7. BSE and reflected light (crossed polars) figures of baumhauerite and argentobaumhauerite aggregates from Lengenbach, Binntal, Switzerland. Abbreviations: bmh – bauhauerite; agbmh – argentobaumhauerite; rth – rathite; srt – sartorite. Exsolutions and replacements illustrated in figures *a–d* are described in the text.

embayments reaching from the boundaries into the grains, is illustrated in Fig. 7*a*.

We ascribe genesis of the argentobaumhauerite aggregates in the form of lamellae and spindles inside the baumhauerite matrix to exsolution processes, and with them connected migration of Ag to the grain boundaries of baumhauerite, with

subsequent replacement of marginal grain portions by argentobaumhauerite. Argentobaumhauerite has been replaced to a different degree by rathite and sartorite (Fig. 7*c*). Both replacement processes show dependence on the crystallographic orientation of the original argentobaumhauerite. Sartorite replaces rathite as well, without regard
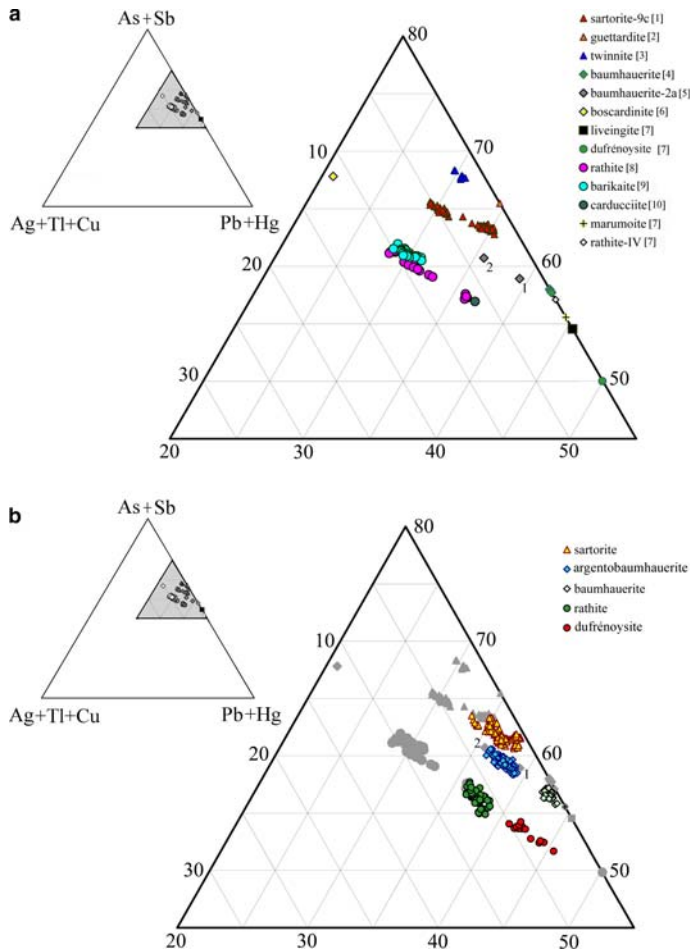
FIG. 8. Composition triangle (Pb + Hg) – (As + Sb) – (Ag + Cu + Tl) (atomic proportions of cations) with (*a*) known minerals of the sartorite homologous series and (*b*) baumhauerite, argentobaumhauerite and associated sartorite homologues from Lengenbach, analysed in the present work. References: [1] Berlepsch *et al.* (2003); [2] Makovicky *et al.* (2012); [3] Makovicky and Topa (2012); [4] Topa (unpublished data); [5] Laroussi *et al.* (1989); [6] Orlandi *et al.* (2012); [7] Moëlo *et al.* (2008); [8] Berlepsch *et al.* (2002); [9] Topa *et al.* (2013); and [10] Biagioni *et al.* (2014). Numbers 1 and 2 in (*a*) and (*b*) indicate 1Ag and 2Ag per formula unit. (i.e. $AgPb_{22}As_{33}S_{72}$ and $Ag_2Pb_{20}As_{34}S_{72}$, respectively). Note: sartorite and dufrénoysite are Ag-, Cu-free, Tl-based phases.

to its orientation (Fig. 7*d*). As a result of the series of exsolutions and replacements, pure mineral grains of sartorite homologues are rare at Lengenbach.

The position of the analysed sartorite homologues from Lengenbach in the Pb – (Ag + Cu + Tl) – (As + Sb) system is illustrated in Fig. 8*a* and *b*. Baumhauerite and argentobaumhauerite occupy the central line of the diagram as two well-separated composition clusters. The As–Sb diagram (Fig. 9*a*) indicates that the As–Sb ratios in baumhauerite and

argentobaumhauerite are a part of a single baumhauerite – rathite – sartorite sequence in which, very broadly, the Sb content is a function of the As content: at.% Sb ≈0.133 at.% As. Dufrenoysite lies outside this trend. The Tl–Ag diagram (Fig. 9*b*) sharply separates the Ag-substitution and the Tl-substitution lines of these sulfosalts. Dufrenoysite matches the low Ag contents observed in baumhauerite from Lengenbach whereas the linear increase of Tl contents from baumhauerite through argentobaumhauerite to rathite does not
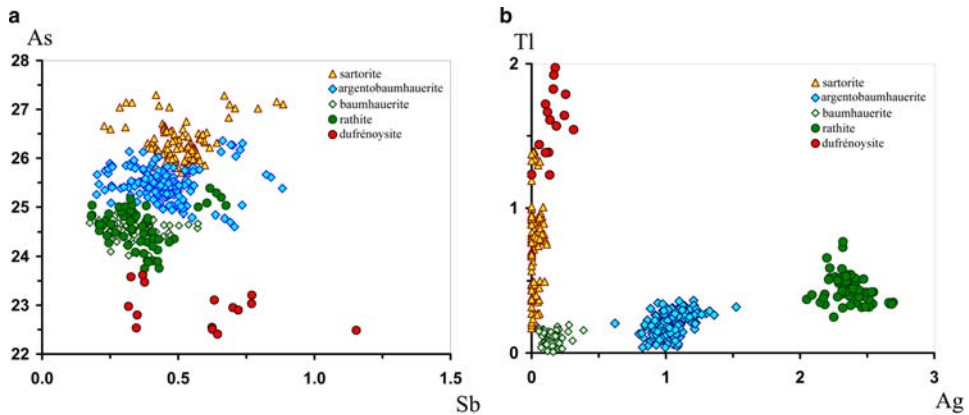
FIG. 9. (*a*) As–Sb and (*b*) Tl–Ag correlations for the sartorite homologues from Lengenbach, present in the baumhauerite samples and analysed in this study. Element concentrations are expressed in atomic percent.

reach even a quarter of the trend observed from sartorite to dufrenoysite. This might indicate that the rathite stage is a continuation of the baumhauerite stage whereas the subsequent sartorite deposition, confirmed by the textural observations described above, and the replacement processes were produced by solutions with a different composition. The position of dufrénoysite is still open. We find it interesting, that philrothite, ideally a nearly pure Tl–As–S phase (Bindi *et al.*, 2014) appears to be a product of a late mineralization phase.

Baumhauerite and argentobaumhauerite are just a part of the deposition sequence of Pb–As sulfosalts at Lengenbach and the above described observations help to fix their position in this sequence. If confirmed by further observations, the separation of Ag enriched and Tl enriched mineralization periods in the deposit is remarkable.

The substitution-free baumahauerite material comes from Moosegg near Grubach, ∼4 km from Golling, Salzburg Land, Austria (Graeser *et al.*, 1986). The sulfide mineralization occurs in association with a gypsum-anhydrite mass which contains inclusions of Werfen slates and altered volcanic rocks, and with marls, limestones and dolomites of Gutenstein formation. A locally developed, thin sulfide horizon contains a baumhauerite-sphalerite mineralization with minor liveingite(?) and/or dufrénoysite(?), enargite, galena, sulfur, pyrite and seligmannite. In the same locality, a galena-sphalerite mineralization also occurs, with pyrite and jordanite. Mineralization is believed to have been formed by the elements concentrated from surrounding sediments.

Conclusions

Argentobaumhauerite is a homeotype of baumhauerite. The difference is expressed as a different ('Ag substituted') composition, a supercell of the baumhauerite cell, and a different arrangement of short As–S bond configurations (crankshaft chains) in the structures. The remarkable unit-cell scale separation of Ag and surplus As into an alternative set of $N = 4$ slabs, creating well localized (Ag + As,Sb) substitution sites, is responsible for the doubling of the *c* parameter. It raises a question whether there exists a pure phase with only silver-substituted $N = 4$ slabs. Structurally, it might face a size misfit between the $N = 3$ and $N = 4$ slabs, which is adjusted easily when every second $N = 4$ slab is Pb rich. The perfection of intra-cell separation of the unsubstituted and extensively substituted portions is quite surprising although the HRTEM observations of Pring *et al.* (1990) reveal that it could also be arrested at different stages of the process.

Argentobaumhauerite is not a polytype of baumhauerite – it is an independent mineral species with its own local (crankshaft chain) configurations and local symmetries (inversion centres instead of complete asymmetry), both very different from baumhauerite, and with cation substitution sites which are not present in baumhauerite. Thus, it is not just presence or absence of inversion relating adjacent structural slabs, but the slabs themselves in the two mineral species are configured differently. It was rather unfortunate that, due to the history of its research, its former name (i.e. baumhauerite-2*a*) resembled a polytype.

The HRTEM observations inevitably do not reach the degree of resolution detail which would illustrate the here described crankshaft chain schemes and substitutions. Thus, the models of Pring and Graeser (1994) were just the first approximation to the true structural situation.

Acknowledgements

References

Berlepsch, P., Makovicky, E. and Balić-Žunić, T. (2001) Crystal chemistry of sartorite homologues and related sulfosalts. *Neues Jahrbuch für Mineralogie Abhandlungen*, **176**, 45–66.

Berlepsch, P., Armbruster, T., Makovicky, E. and Topa, D. (2003) Another step toward understanding the true nature of sartorite: Determination and refinement of a nine-fold superstructure. *American Mineralogist*, **88**, 450–461.

Berlepsch, P., Armbruster, T. and Topa, D. (2002) Structural and chemical variations in rathite, $Pb_8Pb_{4-x}(Tl_2As_2)_x(Ag_2As_2)As_{16}S_{40}$: modulations of a parent structure. *Zeitschrift für Kristallographie*, **217**, 1–10.

Biagioni, C., Orlandi, P., Moëlo, Y. and Bindi, L. (2014) Lead-antimony sulfosalts from Tuscany (Italy). XVI. Carducciite, $(AgSb)Pb_6(As,Sb)_8S_{20}$, a new Sb-rich isotype of rathite from the Pollone mine, Valdicastello Carducci: occurrence and crystal structure. *Mineralogical Magazine*, **78**, 1775–1793.

Bindi, L., Nestola, F., Makovicky, E., Guastoni, A. and De Battisti, L. (2014) Tl-bearing sulphosalts from the Lengenbach quarry, Binn valley, Switzerland: Philrothite, $TlAs_3S_5$. *Mineralogical Magazine*, **78**, 1–9.

Bruker AXS (1997) *XPREP, Version 5.1*, Bruker AXS, Inc., Madison, Wisconsin, USA.

Bruker AXS (1998a) *SMART, Version 5.0*, Bruker AXS, Inc., Madison, Wisconsin, USA.

Bruker AXS (1998b) *SAINT, Version 5.0*, Bruker AXS, Inc., Madison, Wisconsin, USA.

Engel, P. and Nowacki, W. (1969) Die Kristallstruktur von Baumhauerit. *Zeitschrift für Kristallographie*, **129**, 178–202.

Graeser, S., Paar, W.H. and Chen, T.T. (1986) Baumhauerit: ein zweites Vorkommen (Salzburg, Austria). *Schweizerische mineralogische und petrographische Mitteilungen*, **66**, 259–266.

Laroussi, A., Moëlo, Y., Ohnenstetter, D. and Ginderow, D. (1989) Argent et thallium dans les sulfosels de la série de la sartorite (Gisement de Lengenbach, vallée de Binn, Suisse). *Comptes Rendus de l'Académie des Sciences, Paris*, **308**, Série II, 927–933.

Makovicky, E. (1985) The building principles and classification of sulphosalts based on the SnS archetype. *Fortschritte der Mineralogie*, **63**, 45–89.

Makovicky, E. (1997a) Modular crystal chemistry of sulphosalts and other complex sulphides. Pp. 237–271 in: *Modular Aspects of Minerals* (S. Merlino, editor). European Mineralogical Union, Notes in Mineralogy, **1**. Eötvös University Press, Budapest.

Makovicky, E. (1997b) Modularity – different types and approaches. Pp. 315–343 in: *Modular Aspects of Minerals* (S. Merlino, editor). European Mineralogical Union, Notes in Mineralogy, **1**. Eötvös University Press, Budapest.

Makovicky, E. and Topa, D. (2012) Twinnite, $Pb_{0.8}Tl_{0.1}Sb_{1.3}As_{0.80}S_4$, the OD character and the question of its polytypism. *Zeitschrift für Kristallographie*, **227**, 468–475.

Makovicky, E. and Topa, D. (2014) The crystal structure of jasrouxite, a Pb-Ag-As-Sb member of the lillianite homologous series. *European Journal of Mineralogy*, **26**, 145–155.

Makovicky, E. and Topa, D. (2015) Crystal chemical formula for sartorite homologues. *Mineralogical Magazine*, **79**, 25–31.

Makovicky, E., Topa, D., Tajjedin, H., Rastad, E. and Yaghubpur, A. (2012) The crystal structure of guettardite, $PbAsSbS_4$. *The Canadian Mineralogist*, **50**(2), 253–265.

Marumo, F. and Nowacki, W. (1965) The crystal structure of rathite-I. *Zeitschrift für Kristallographie*, **122**, 433–456.

Marumo, F. and Nowacki, W. (1967) The crystal structure of dufrénoysite, $Pb_{16}As_{16}S_{40}$. *Zeitschrift für Kristallographie*, **124**, 409–419.

Moëlo, Y., Makovicky, E., Mozgova, N.N., Jambor, J.L., Cook, N., Pring, A., Paar, W.H., Nickel, E.H., Graeser, S., Karup-Møller, S., Balić-Žunić, T., Mumme, W.G., Vurro, F., Topa, D., Bindi, L., Bente, K. and Shimizu, M. (2008) Sulfosalt systematics: a review. Report of the sulfosalt sub-committee of the IMA Commission on Ore Mineralogy. *European Journal of Mineralogy*, **20**, 7–46.

Orlandi, P., Biagioni, C., Bonaccorsi, E., Moëlo, Y. and Paar, W.H. (2012) Lead-antimony sulfosalts from Tuscany (Italy). XII. Boscardinite, $TlPb_3(Sb_7As_2)_{\Sigma9}S_{18}$, a new mineral species from the Monte Arsiccio mine: occurrence and crystal structure. *The Canadian Mineralogist*, **50**, 235–251.

Pring, A. (2001) The crystal chemistry of the sartorite group minerals from Lengenbach, Binntal, Switzerland – a HRTEM study. *Schweizerische mineralogische und petrographische Mitteilungen*, **81**, 69–87.

Pring, A. and Graeser, S. (1994) Polytypism in baumhauerite. *American Mineralogist*, **79**, 302–307.

Pring, A., Birch, W.D., Sewell, D., Graeser, S., Edenharter, A. and Criddle, A. (1990) Baumhauerite-2*a*: A silver-bearing mineral with a baumhauerite-like supercell from Lengenbach, Switzerland. *American Mineralogist*, **75**, 915–922.

Sheldrick, G.M. (1997*a*) *SHELXS-97. A computer program for crystal structure determination*. University of Göttingen, Germany.

Sheldrick, G.M. (1997*b*) *SHELXL-97. A computer program for crystal structure refinement*. University of Göttingen, Germany.

Solly, R.H. (1902) Sulpharsenites of lead from the Binnenthal. Part III. Baumhauerite, a new mineral; and dufrenoysite. *Mineralogical Magazine*, **13**, 151–171.

Topa, D., Makovicky, E., Tajedin, H., Putz, H. and Zagler, G. (2013) Barikaite, $Ag_3Pb_{10}(Sb_8As_{11})_{\Sigma19}S_{40}$, a new member of the sartorite homologous series. *Mineralogical Magazine*, **77**, 3039–3046.